PHYSICAL REVIEW D VOLUME 22, NUMBER 5 1 SEPTEMBER 1980

Heavy-quark–antiquark potential in the MIT bag model

W. C. Haxton and L. Heller
Theoretical Division, Los Alamos Scientific Laboratory, University of California, Los Alamos, New Mexico 87545
(Received 27 March 1980)

The MIT bag model for a meson composed of a heavy quark and a heavy antiquark is solved using the Born-Oppenheimer approximation. For fixed $q\bar{q}$ separations the color-electric fields and bag shapes are determined by solving numerically the Yang-Mills equations with bag boundary conditions to lowest order in the quark-gluon coupling constant. Spin effects are not included. The resulting bag energy is used as a potential energy in the Schrödinger equation for the relative motion of the quarks. Good agreement with the experimental ψ and Υ spectra and leptonic decay widths is found. When the same potential is applied to strange-quark systems, a consistent picture of the masses of the ϕ and F^* mesons emerges. The relation between spectroscopy and the variation of the coupling constant with distance is explored.

INTRODUCTION

The physical picture which emerged from the MIT bag-model[1] description of the light hadrons is that of light quarks u, d, and s moving relativistically throughout the entire bag volume. The quarks are allowed to occupy the lowest mode for the free Dirac field in a spherical cavity. The zeroth-order (in the color coupling constant) contribution to the hadron energy is the sum of the eigenvalues of these quarks, the bag volume energy, and the zero-point energies. To this is added the interaction of the quarks with the color electric and magnetic fields, calculated in second-order perturbation theory.[2]

In this paper we apply the bag model to heavy mesons composed of b and c quarks. Here a very different description, in which the gluon field adjusts rapidly with respect to the motion of the heavy quarks, is appropriate. Our treatment is based on a Born-Oppenheimer approximation with the quark-antiquark separation treated as an adiabatic variable.[3,4] We first solve, to lowest order in the coupling constant, the Yang-Mills equations for the gluon field generated by static sources. In order to satisfy the bag boundary conditions, both the bag surface and the color-electric field must be determined simultaneously. The resulting bag energy is then regarded as a potential for describing the relative motion of the quarks. Since we neglect the color spin, only the central part of the potential is obtained. We find the lowest eigenvalues and eigenfunctions for this potential by solving the Schrödinger equation. Apart from the quark masses, the only adjustable parameters in this treatment are the two that describe the variation of the running coupling constant with distance.

Our work is presented as follows. In Sec. I we discuss the parameters of the MIT bag model and the expected variation of the coupling constant with distance. Our method of solving the bag problem for two fixed sources is described. We present numerical results in Sec. II, including the quark-antiquark potential as a function of separation, the bag shape, and the configuration of the color fields. In Sec. III we use this potential to generate spectra and leptonic decay widths for the ψ and Υ systems. We also treat intermediate mass mesons having one or more strange quarks. In the concluding section we compare the adiabatic and "fixed-bag"[1,2,5] approximations to the MIT bag model, and discuss some previous phenomenological treatments of the q-$\bar{q}$ potential.

I. THE STATIC-BAG PROBLEM

There are four parameters in the MIT bag-model calculation of the light hadrons: the bag volume constant B, the color coupling constant α, a zero-point energy coefficient Z_0, and the mass m_s of the strange quark. The numerical values of these parameters were fixed[2] by fitting to the masses of four particles ω, N, Δ, and Ω^-. Additional properties of these particles and the characteristics of other light hadrons were then predicted. The typical size of bag radii and interquark separations in these calculations is 1 fm.

In applying this model to the $c\bar{c}$ and $b\bar{b}$ systems, in which the quark separations are much smaller, we must ask whether these parameters are expected to have the values determined from the light hadrons. Since the bag constant B describes properties of the vacuum, its value should be independent of the quark configuration, so we adopt the MIT value $B^{1/4}=0.145$ GeV. The light-hadron zero-point energy was represented by a phenomenological term of the form $-Z_0/R_0$, with R_0 the spherical bag radius and with $Z_0=1.84$. This picture of the zero-point energy of the quantum fields confined in a bag now appears to be incomplete.[6,7]

However, lacking a better prescription, we will use the same form for the zero-point energy, with R_0 the radius of the best spherical approximation to our more complicated bags. We will fix the strange quark mass in Sec. III when we discuss the ϕ and F^* mesons.

We expect the remaining parameter, α, to have a strong dependence on the q-$\bar{q}$ separation, since asymptotic freedom predicts a weakening of the color coupling constant at small distances according to[8]

$$\frac{g^2}{4\pi} \equiv \alpha(r) \underset{r\to 0}{\to} \frac{4\pi}{11-\frac{2}{3}n_f} \frac{1}{\ln(1/\Lambda^2 r^2)}, \tag{1}$$

with r the separation of the quark and antiquark. Here Λ is a scale constant and n_f is the number of quark flavors. (We choose $n_f=3$ since the Compton wavelengths of the heavier $q\bar{q}$ pairs are appreciably smaller than the size of the systems we are considering.[9]) The limiting behavior as $r\to 0$ is not sufficient to specify $\alpha(r)$; indeed, Eq. (1) becomes infinite when $r=\Lambda^{-1}$. A constraint at a finite value of r is available from the bag-model calculations of the light hadrons,[2] which yielded a value $\alpha=2.2$. Consequently we intended to assume a form for the running coupling constant $\alpha(r)$ which is consistent with the limiting behavior of Eq. (1) and for which $\alpha(1\text{ fm})=2.2$. A simple function obeying these constraints is

$$\alpha(r)=\frac{4\pi}{11-\frac{2}{3}n_f}\frac{1}{\ln(\gamma+1/\Lambda^2 r^2)}, \tag{2}$$

where, for a given value of the scale constant, γ is fixed so that $\alpha(1\text{ fm})=2.2$. However, as we will discuss in more detail later, we could only obtain a fair representation of the $c\bar{c}$ spectrum with this approach. Relaxing the constraint at $r=1$ fm, we found excellent agreement with experimental spectra could be obtained for smaller values of $\alpha(1\text{ fm})$. Effectively, then, we have employed Eq. (2) with both γ and Λ independent parameters.

With the bag-model parameters so fixed, we proceed to the first stage of the Born-Oppenheimer approximation described in the Introduction, solving the Yang-Mills equations in the interior of the bag for a quark color charge density

$$\rho^a(\vec{x})=g(r)[F^a(1)\delta^{(3)}(\vec{x}-\vec{r}_1)+F^a(2)\delta'^{(3)}(\vec{x}-\vec{r}_2)] \tag{3}$$

and no current density. $F^a(1)=\lambda^a/2$ is the SU(3)-color generator for a quark and $F^a(2)$ the generator for an antiquark. Following Ref. 4 we find to relative order g^4 that $\vec{E}^a=-\vec{\nabla}\phi^a$ and that the equations for the different color components uncouple. Since the transverse degrees of freedom of the gluon field are assumed to be unexcited, the quark and antiquark state is a color singlet, for which $F^a(2)=-F^a(1)$. A solution of the form $\phi^a(\vec{x})=(\lambda^a/2)\phi(\vec{x})$ can then be obtained in which Poisson's equation

$$\nabla^2\phi(\vec{x})=-g(r)[\delta^3(\vec{x}-\vec{r}_1)-\delta^3(\vec{x}-\vec{r}_2)]\equiv-\rho(\vec{x}) \tag{4}$$

must be solved subject to the bag boundary conditions

$$\hat{n}\cdot\vec{E}^a=0 \tag{5a}$$

and

$$\tfrac{1}{2}\sum_a(\vec{E}^a)^2=B. \tag{5b}$$

The magnetic contribution to Eq. (5b) is of relative order g^4 and thus has been ignored.

To solve the problem posed by Eqs. (4) and (5) we must determine simultaneously the bag surface and the field ϕ. Matters are complicated by the fact, following from the boundary conditions, that the surface contains two singular points.[10] Although the two-dimensional analog of this problem can be solved analytically by conformal mapping,[11] the present case must be treated numerically. Our approach is to assume a set of trial surfaces, given by an analytic form having several adjustable parameters and the required cusps, and to solve Eq. (4) exactly and satisfy the boundary conditions approximately by a technique based on Green's theorem. The parameters specifying that surface which allows us to best satisfy Eqs. (5) are then determined by a minimization procedure. An alternative, and equivalent, procedure would be to satisfy Eqs. (4) and (5a) exactly on a trial surface, and then vary that surface to minimize the sum of the electric and volume energies. We believe this second approach would be less advantageous numerically.

Our starting point is a formal expression for the potential at an arbitrary interior point $\vec{x}$ in terms of volume and surface integrals

$$4\pi\phi(\vec{x})=\int dV'\frac{\rho(\vec{x}')}{|\vec{x}'-\vec{x}|}+\int dS'\left[\frac{1}{|\vec{x}'-\vec{x}|}\hat{n}'\cdot\vec{\nabla}'\phi(\vec{x}')-\phi(\vec{x}')\hat{n}'\cdot\vec{\nabla}'\frac{1}{|\vec{x}'-\vec{x}|}\right]. \tag{6}$$

For the correct surface, $\hat{n}'\cdot\vec{\nabla}'\phi$ is zero by Eq. (5a). Equation (5b) requires

$$(\vec{\nabla}\phi)^2=\frac{2B}{\sum_a(\lambda^a/2)^2}\equiv G^2 \tag{7}$$

on the surface. Note that $\sum_a(\lambda^a/2)^2=\frac{4}{3}$. We adopt a spherical coordinate system with origin at the midpoint of the two quarks and with the axis along

the line determined by the quarks, and look for an axially symmetric solution of Eq. (6). Equation (7), when combined with Eq. (5a), then allows us to write

$$\phi(\vec{x}) = GS(\theta) \tag{8}$$

for all points on the bag boundary. Here $S(\theta)$ is the arc length along the surface, which, in order to preserve reflection symmetry about the equatorial plane, we choose so that $S(\theta) = -S(\pi - \theta)$. Equation (6) can now be written as

$$4\pi\phi(\vec{x}) = \int dV' \frac{\rho(\vec{x}')}{|\vec{x}' - \vec{x}|} - G\int dS' S(\theta')\hat{n}' \cdot \vec{\nabla}' \frac{1}{|\vec{x}' - \vec{x}|} . \tag{9}$$

Using the charge density of Eq. (4), the volume integral can be evaluated analytically, while the azimuthal part of the surface integral can be written in terms of the elliptic integrals E and D. Subsequent differentiation of this expression yields a corresponding, though more complicated, formula for $\vec{\nabla}\phi$. These results are presented in the Appendix.

For any bag boundary Eq. (9) will yield a function $\phi(\vec{x})$ obeying Poisson's equation. Using the analogous expression for $\vec{\nabla}\phi(\vec{x})$, we can let $\vec{x}$ approach the surface to check the boundary conditions [Eqs. (5)], neither of which, in general, will be satisfied. Thus, to determine an optimal surface, we define a positive-definite measure of the degree to which Eqs. (5) are not satisfied,[12]

$$\Delta \equiv \frac{1}{G^2} \frac{\int dS\{[\hat{n} \cdot \vec{\nabla}\phi(\vec{x})]^2 + [|\vec{\nabla}\phi(\vec{x})| - G]^2\}}{\int dS} , \tag{10}$$

and minimize this quantity as a function of the parameters determining the surface. If Δ can be forced to zero, then an exact solution has been found. This minimization procedure is not totally satisfactory, of course, since computationally only local minima are determined. We have repeated this minimization for many starting values of the surface parameters, however, to gain a more global view of the parameter space.

Generally we have restricted our surfaces to three- and four-parameter forms. Our most successful guesses in terms of minimizing Δ are

$$R_1(\theta) = \frac{\bar{R}(1 + \beta \sin^p \theta)}{[1 + (\tan^2\theta_0 - 1)\cos^2\theta]^{1/2}} \tag{11a}$$

and

$$R_2(\theta) = \frac{\bar{R}(1 + \beta \sin^p \theta e^{-\sin\theta/\sin\theta_0})}{[1 + (\tan^2\theta_0 - 1)\cos^2\theta]^{1/2}} , \tag{11b}$$

with the parameters to be varied being $\bar{R}$, θ_0, β, and p. $R_2(\theta)$ is the better choice for q-$\bar{q}$ separations greater than 1.2 fm. Each of these surfaces can go to spherical and cylindrical limits. The values determined for Δ range from approximately 3.5×10^{-5} at small separations to 2.4×10^{-4} at $r = 2.5$ fm. For comparison, optimal spherical bags yield values between 0.008 and 0.12.

Following this minimization the bag energy can be determined as a function of r

$$E(r) = \int dV[\tfrac{1}{2}\tfrac{4}{3}(\vec{\nabla}\phi)^2 + B] . \tag{12}$$

The infinite self-energy terms are removed from Eq. (12) analytically; these are, of course, independent of r. $E(r)$ is regarded, in the second part of the Born-Oppenheimer approximation, as a potential energy for the relative motion of the q-$\bar{q}$ pair. The effective Hamiltonian for this motion is

$$H(r) = m_1 + m_2 + \frac{\vec{p}^2}{2\mu} + V(r) , \tag{13}$$

with m_1 and m_2 the masses of the quark and antiquark, μ the reduced mass, and $V(r)$ equal to the sum of $E(r)$ and the zero-point energy. The Schrödinger equation is solved for this Hamiltonian, yielding the eigenvalues and eigenfunctions of the $q\bar{q}$ system.

In the next section we will give our numerical results for $E(r)$, explain the accuracy checks we have performed, and show bag surfaces and field configurations for selected q-$\bar{q}$ separations.

II. NUMERICAL RESULTS FOR $E(r)$

As we mentioned earlier, asymptotic freedom implies a quenching of the color coupling constant α as $r \to 0$. Using the constraint $\alpha(1\text{ fm}) = 2.2$ from the MIT bag calculation of the light hadrons and the phenomenological form for $\alpha(r)$ given by Eq. (2), $E(r)$ can be calculated once the scale constant Λ is fixed. Although we will postpone our discussion of $b\bar{b}$ and $c\bar{c}$ spectroscopy until Sec. III, Λ has been determined by comparing our predictions for the $2s$-$1s$ and $1p$-$1s$ splittings in charmonium to the experimental values. We have tested values of Λ between 0.2 and 0.8 GeV. Although the choice $\Lambda = 0.375$ GeV nicely reproduces these two splittings, serious discrepancies occur for the higher states in charmonium.[13] (This will be shown in Sec. III.) However, on relaxing the constraint that α (1 fm) = 2.2, we found marked improvement could be obtained with weaker coupling constants. Most of the results of this section will be given for $\alpha(1\text{ fm}) = 1.0$ and $\Lambda = 0.240$ GeV (thus $\gamma = 3.364$). This running coupling constant is compared to that obtained with $\alpha(1\text{ fm}) = 2.2$ and $\Lambda = 0.375$ (thus $\gamma = 1.609$) in Fig. 1.

Using this running coupling constant we have followed the numerical program described in the pre-

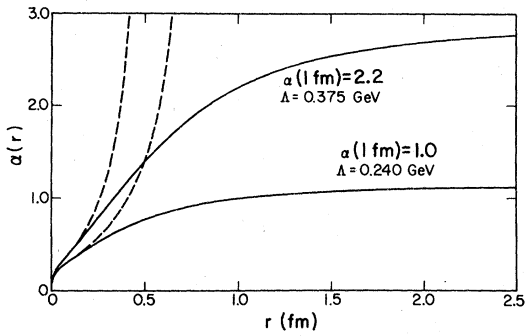

FIG. 1. Comparison of the running coupling constant of Eq. (2) for the constraints $\alpha(1\text{ fm})=2.2$ and $\alpha(1\text{ fm})=1.0$. The scale constants Λ were determined by fitting the $1p-1s$ splittings in charmonium. The dotted curves are the simple asymptotic freedom forms [Eq. (1)] for these same scale constants.

vious section for quark separations ranging from 0.01 to 2.5 fm. Our results for a q-$\bar{q}$ separation of 0.3 fm, which is approximately the location of the peak of the $\psi(3095)$ relative wave function, is given in Fig. 2. Here the bag shape, the color field ϕ, and the electric field $-\vec{\nabla}\phi$ are shown graphically. We also describe, in Fig. 3, the evolution of the shape of the bag as the quark separation increases. For separations $r \gtrsim 1.5$ fm the singular behavior of the cusps [i.e., for the surfaces given in Eqs. (11), the parameter p being less than unity] has been lost. Though this implies some error in enforcing the boundary conditions near the cusps, this result is not unexpected due to the limitations of the trial surfaces we have employed. Figure 3 illustrates that, even for large separations, the bag is far from the asymptotic cylindrical limit.

The bag-volume energy $E_{\text{VOL}}(r)$ and the electric-field energy $E_{\text{EL}}(r)$ contributions to $E(r)$ [see Eq. (12)] are given in Fig. 4. The zero-point energy $E_0(r)=-1.84/R_0(r)$, where R_0 is the radius of the best spherical approximation to the bag, is also shown. The electric energy has the expected Coulomb behavior at small separations, while at large separations both contributions to $E(r)$ are growing nearly linearly. To illustrate this we write

$$E(r)=-\frac{4}{3}\frac{\alpha(r)}{r}+\left[\frac{32\pi B\alpha(r)}{3}\right]^{1/2}r+Q(r). \quad (14)$$

The first two terms are the Coulomb and "linear" confining terms which we know to be appropriate in the $r\to 0$ and $r\to\infty$ infinite cylinder limits, respectively. In Fig. 5 we decompose $E(r)$ in the manner of Eq. (14) in order to show the bag-model prediction for the function which interpolates between these limits, $Q(r)$. Though growing almost

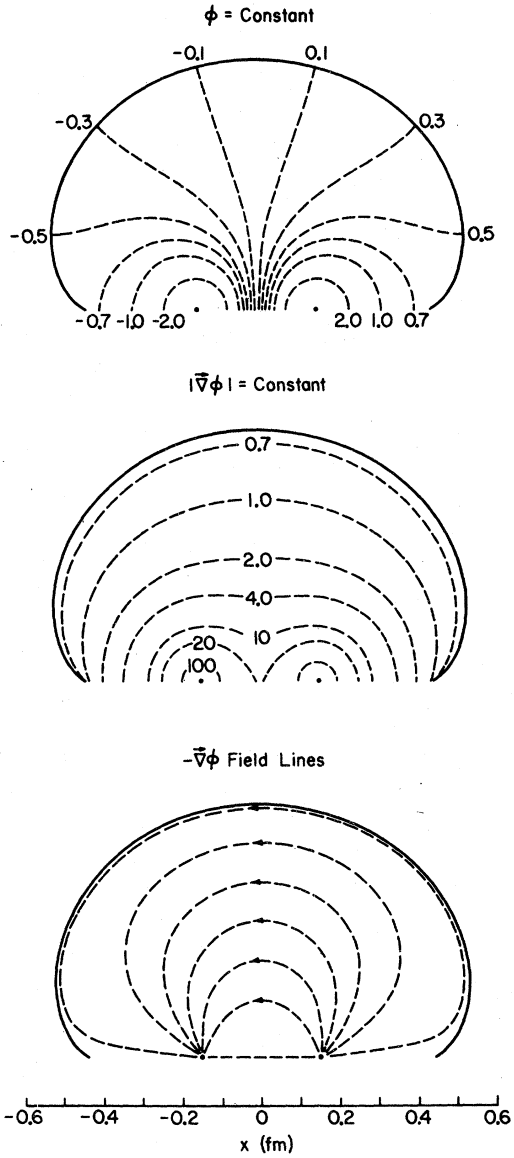

FIG. 2. The bag shape, equipotential surfaces (in fm^{-1}), surfaces where the magnitude of the electric field is constant (in fm^{-2}), and the direction of the electric field are shown for a q-$\bar{q}$ separation of 0.3 fm. The coupling constant is $\alpha(0.3\text{ fm})=0.585$.

linearly for small q-$\bar{q}$ separations, $Q(r)$ flattens out at large r. A finite-cylinder approximation to the bag for large separations predicts

$$Q_{\text{cyl}}(r)\simeq C[B\alpha^3(r)]^{1/4} \quad (15)$$

with $C=-0.90$.[14] For $\alpha(2.5\text{ fm})=1.12$, $Q_{\text{cyl}}(2.5\text{ fm})=-0.142$ GeV, which can be compared to our result of $Q(2.5\text{ fm})=-0.158$ GeV.

Our solutions to the problem formulated in the previous section are not exact, owing to the small number of parameters describing our trial bags,

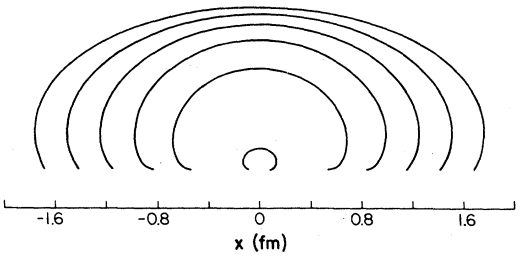

FIG. 3. The bag shapes corresponding to q-$\bar{q}$ separations of 0.01, 0.5, 1.0, 1.5, 2.0, and 2.5 fm are shown. The coupling-constant parameters [Eq. (2)] are $\Lambda = 0.24$ GeV and $\alpha(1\text{ fm}) = 1.0$.

although systematic improvements to these results are numerically straightforward. Thus we need methods of estimating the discrepancy between our results and an exact solution. One check is provided by a generalization of the energy scaling relation of Ref. 15 for the case of a running coupling constant. For couplings such that $\alpha(0)=0$, this relation can be written

$$E^{\mathrm{SC}}(r)=\frac{4}{r}\int_0^r dr' E_{\mathrm{VOL}}(r') + \frac{1}{r}\int_0^r dr' r' E_{\mathrm{EL}}(r')\frac{\partial}{\partial r'}\ln\alpha(r'), \quad (16)$$

where $E^{\mathrm{SC}}(r)=E_{\mathrm{VOL}}(r)+E_{\mathrm{EL}}(r)$ for the exact solution. A comparison of $E(r)$ and $E^{\mathrm{SC}}(r)$ is made in Table I, where differences are shown to be of the order of 0.1%. We stress that Eq. (16) is only a consistency check; however, the simple spherical-bag approximation fails this test badly for q-$\bar{q}$ separations greater than 1 fm.

A second test is provided by partially integrating Eq. (12), using Poisson's equation, and then assuming boundary condition Eq. (5a) is satisfied exactly. We find

$$E^{\mathrm{BC}}(r)=B\int dV+\tfrac{2}{3}g(r)[\phi(1)-\phi(2)], \quad (17)$$

where $\phi(1)$ and $\phi(2)$ are the potentials at the positions of the quark and antiquark. The infinite self-energy subtraction made here is identical to that made in Eq. (12). A comparison of $E^{\mathrm{BC}}(r)$ and $E(r)$ also is given in Table I. While agreement is

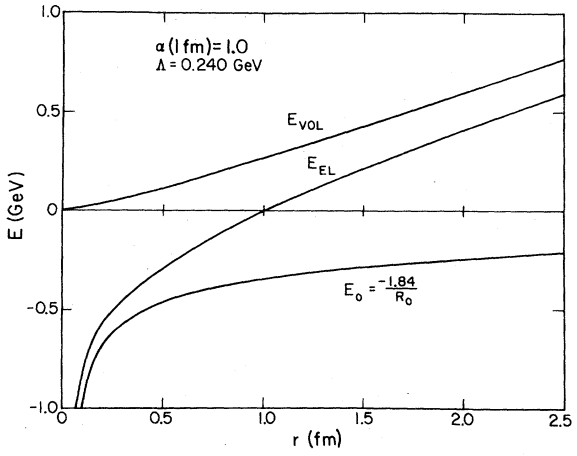

FIG. 4. Decomposition of the bag energy $E(r)$ into its volume $E_{\mathrm{VOL}}(r)$ and electric $E_{\mathrm{EL}}(r)$ components. The zero-point energy for $Z_0 = 1.84$ is also shown.

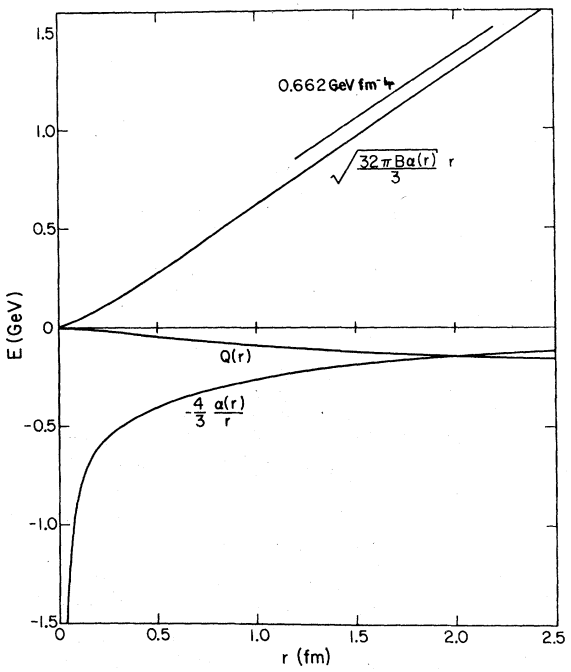

FIG. 5. Decomposition of the sum of the electric and volume energies according to Eq. (14), showing the Coulomb term, the "linear" confining term, and the remainder $Q(r)$. The straight line segment indicates the asymptotic slope of the linear term.

TABLE I. The bag energy $E(r)$ calculated for α (1 fm) = 1.0 and $\Lambda = 0.240$ GeV is compared to $E^{\mathrm{SC}}(r)$ of Eq. (16), to $E^{\mathrm{BC}}(r)$ of Eq. (17), and to $E^{\mathrm{SPH}}(r)$ corresponding to the best spherical approximation to the bag. Also shown is $\Delta(r)$, defined in Eq. (10), which measures the degree to which the boundary conditions have not been satisfied. All energies are given in GeV.

r (fm)	$E(r)$	$E^{\mathrm{SC}}(r)$	$E^{\mathrm{BC}}(r)$	$E^{\mathrm{SPH}}(r)$	$\Delta(r)$
0.01	−4.163		−4.163	−4.163	4.16×10^{-5}
0.1	−0.833		−0.833	−0.832	3.63×10^{-5}
0.3	−0.396	−0.396	−0.397	−0.396	4.04×10^{-5}
0.5	−0.181	−0.181	−0.184	−0.184	4.36×10^{-5}
1.0	0.264	0.264	0.257	0.271	6.02×10^{-5}
1.5	0.648	0.649	0.637	0.747	1.01×10^{-4}
2.0	1.008	1.008	0.992	1.360	1.49×10^{-4}
2.5	1.357	1.358	1.336	2.199	2.40×10^{-4}

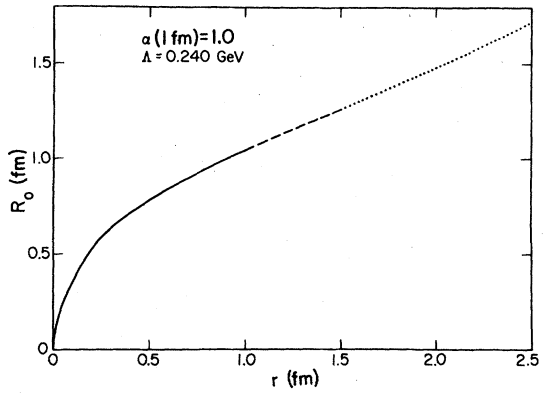

FIG. 6. The radius R_0 of the optimal spherical bag, in terms of minimizing $\Delta(r)$, is given as a function of r. Separations where the spherical-bag energy differs from the full calculation by more than 0.01 GeV and 0.1 GeV are denoted by dashed and dotted lines, respectively.

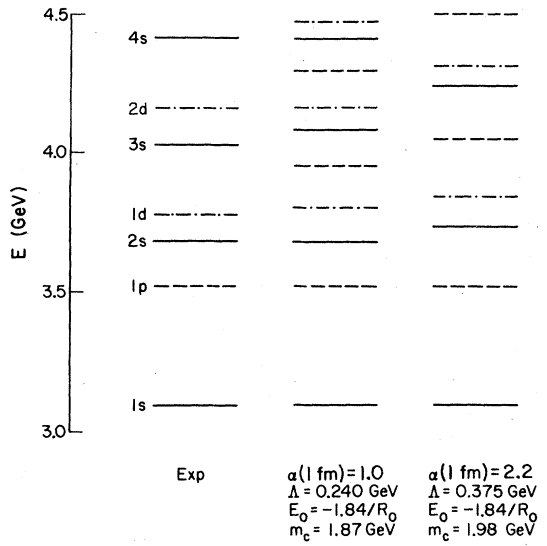

FIG. 7. The experimental spectrum for charmonium is compared to our bag calculation prediction (second column). Also shown are the results of the analogous calculation for $\alpha(1\text{ fm})=2.2$. The experimental p-state energy is the spin-orbit average of the $J=0$, 1, and 2 levels. Solid, dashed, and dash-dotted lines are used for s-, p-, and d-state levels, respectively.

extremely good at small q-$\bar{q}$ separations, this deteriorates somewhat at larger r, correlating with the growing value of $\Delta(r)$. However, even for such r, the discrepancies are on the order of 2%. This, and the energy scaling relation results, have led us to the conclusion that little improvement in $E(r)$ would result from using trial bag surfaces more complicated than those of Eqs. (11).

Also shown in Table I are energies $E^{\mathrm{SPH}}(r)$ generated by the best spherical approximation to the bag boundary. In Fig. 6 the radii of these bags, needed in calculations of the zero-point energy, are given, and q-$\bar{q}$ separations where $E^{\mathrm{SPH}}(r) - E(r)$ exceeds 0.01 and 0.1 GeV are indicated. The analytic expression for this radius in the limit of small r is[4]

$$R_0(r)=\left(\frac{\alpha(r)r^2}{\pi B}\right)^{1/6}. \tag{18}$$

Equation (18) underestimates the numerical result shown in Fig. 6 by approximately 5% at $r=1.0$ fm and 14% at $r=2.0$ fm.

In the next section we will present our results for the spectra, wave functions, and leptonic decay widths of the $c\bar{c}$ and $b\bar{b}$ systems. We also extend this work to the $b\bar{c}$, $c\bar{s}$, $s\bar{s}$, and $b\bar{s}$ systems and consider the appropriateness of a static-potential description for those mesons which contain a strange quark.

III. SPECTROSCOPY

The bag-model prediction for the charmonium spectrum has been determined by numerically solving Schrödinger's equation with the Hamiltonian of Eq. (13). We have previously described the procedure for determining the form of the running coupling constant. The only remaining parameter is the charmed-quark mass $m_1=m_2=m_c$, which we adjust so that the mass of the lowest 1s state agrees with experiment,[16] $m_{\psi/J}=3.095$ GeV. We find $m_c=1.874$ GeV. The known excited $c\bar{c}$ levels are reproduced quite nicely, with the largest discrepancy being the prediction for the ψ'', 0.06 GeV too high. These results are given in Fig. 7. Also shown is the best spectrum we were able to obtain under the constraint that $\alpha(1\text{ fm})=2.2$. One should bear in mind that these spectra depend on the zero-point energy $-Z_0/R_0(r)$. Removing that contribution to the potential energy results in a compression of the energy levels shown in Fig. 7. Thus if Z_0 is changed, or if a different approximation to the zero-point energy is used, we would need different values for Λ and γ in order to reproduce the experimental masses.

The analogous results for $b\bar{b}$ are given in Fig. 8. We find a b-quark mass of 5.265 GeV places the Υ meson at the proper mass, 9.460 GeV. The predicted 2s and 3s states are in reasonable agreement with experiment.

From the Van Royen–Weisskopf formula[17] one can calculate the leptonic decay widths for these vector mesons. As discussed by Richardson,[18] the large corrections in order α to this zeroth-order formula suggest, however, that only the ratios of decay widths can be calculated reliably. Such ratios can be written

$$\frac{\Gamma(V'\to e^+e^-)}{\Gamma(V\to e^+e^-)}=\left|\frac{M_{V'}\psi_{V'}(0)}{M_V\psi_V(0)}\right|^2, \tag{19}$$

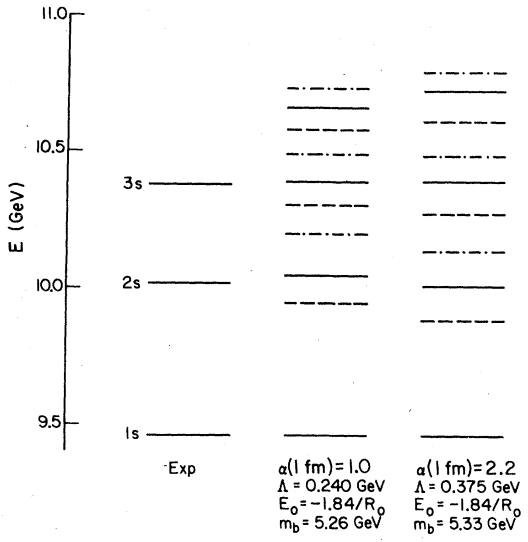

FIG. 8. As in Fig. 7, only for the b-$\bar{b}$ system.

where $\psi_V(0)$ is the vector-meson wave function at the origin. We find using the wave functions we have generated

$$\frac{\Gamma(\psi' \to e^+e^-)}{\Gamma(\psi \to e^+e^-)} = 0.436\,, \quad \frac{\Gamma(\Upsilon' \to e^+e^-)}{\Gamma(\Upsilon \to e^+e^-)} = 0.365\,,$$

while the corresponding experimental values are 0.4 ± 0.1 and 0.3 ± 0.2.[19,20]

The $E1$ transition rates for $\psi' \to \gamma\, ^3P_J$ can be computed from

$$\omega^{^3S_1 \to ^3P_J} = \alpha k \tfrac{16}{27}(2J+1) \times \left\{ \int \left[\frac{kr}{2} j_0\left(\frac{kr}{2}\right) - j_1\left(\frac{kr}{2}\right) \right] u_1^*(r) u_0(r)\, dr \right\}^2$$

with u_1 and u_0 the p- and s-state radial wave functions. The resulting widths are 49.0, 43.0, and 33.5 keV for the $J=0$, 1, and 2 states, respectively. The corresponding experimental widths are 16 ± 9, 16 ± 8, and 16 ± 9 keV. The origin of the discrepancy between theory and experiment is unclear.

In Fig. 9 the wave functions for some of those $c\bar{c}$ and $b\bar{b}$ states whose experimental analogs are known are superimposed on the potential $V(r)$. The corresponding eigenvalues (without the quark masses) are indicated. This figure shows the sensitivity of these states to various ranges of the q-$\bar{q}$ potential.

The concept of a static potential requires that the quark motion be nonrelativistic. A check of this for the systems under considerations is provided by calculating the expectation value of $\langle p^2/m^2 \rangle$. The results for the Υ and ψ mesons, 0.072 and 0.178, are suitably small. We have extended our calculations to the $s\bar{s}$ system, fitting

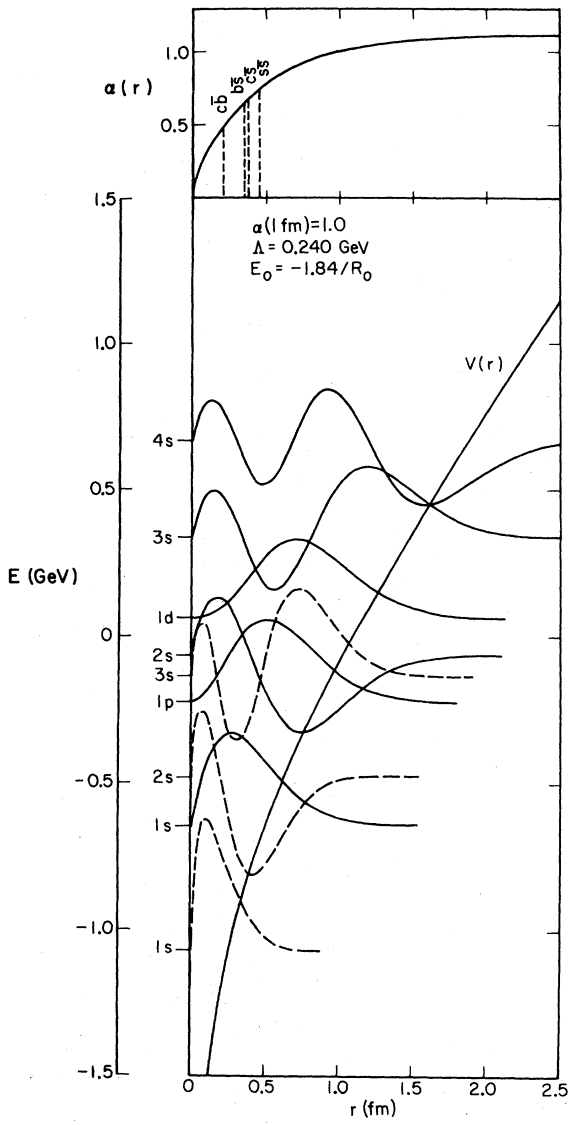

FIG. 9. Calculated wave functions and eigenvalues for several states in the $c\bar{c}$ (solid lines) and $b\bar{b}$ (dashed lines) systems are overlaid on the potential $V(r)$ of Eq. (13). In the top part of the graph the positions of the peaks of the 1s wave functions for the $c\bar{b}$, $b\bar{s}$, $c\bar{s}$, and $s\bar{s}$ systems are shown relative to $\alpha(r)$.

$m_s = 0.641$ GeV to the observed meson mass $M_\phi = 1.02$ GeV. Here $\langle p^2/m^2 \rangle = 0.563$, so that a static-potential approach is on somewhat shakier ground.[21] The predicted $s\bar{s}$ spectrum is given in Fig. 10. Experimental candidates for excited states of the $s\bar{s}$ system have masses 1.470, 1.812, and 2.130 GeV.[22]

With the b, c, and s quark masses determined we can predict the masses of new vector mesons, such as $c\bar{b}$, $b\bar{s}$, and $c\bar{s}$ (the F^* meson). The F^* mass, 2.11 GeV, is consistent with the experimental value of 2.15 ± 0.05 GeV. Other results

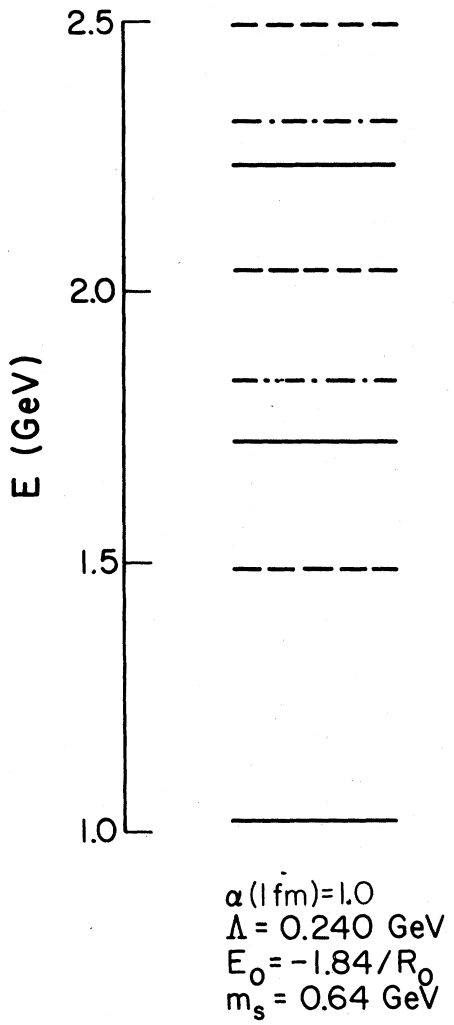

FIG. 10. The calculated spectrum for the $s\bar{s}$ system. Only the ground-state mass, 1.02 GeV, is firmly identified experimentally.

are given in Table II.

It is interesting to compare the present adiabatic approximation to the MIT bag model with the original "fixed-bag" approximation,[1,2] where in lowest order the quarks in the light hadrons are treated as free Dirac fields. Our calculation of $\langle p^2/m^2\rangle$ provides direct evidence, in the adiabatic approximation, for the breakdown of the concept of a static potential for small quark masses. There is also circumstantial evidence of a similar breakdown in the fixed-bag approach when that approximation is applied to heavier quarks: The ψ'-ψ splitting comes out much too small in the work of Ref. 5. Thus possibly the strange-quark mass marks a borderline area for both approaches.

In Table II we also show various contributions to the masses of the vector mesons, some of which have been treated in both the adiabatic and fixed-bag approximations. We note that, despite the larger mass of the strange quark in our calculation, both approaches yield essentially identical values for the mass of the F^* meson. Comparing the expectation values for the zero-point energies E_0 and volume energies $E_{\rm VOL}$, we find our treatment leads to somewhat smaller bags, and consequently larger zero-point energies. The bag electric energies are very different, however. In the fixed-bag approximation, if the quark and antiquark have identical masses, then their zeroth-order wave functions within the bag have the same distribution, so that the electric energy, calculated in second-order perturbation theory, is zero. Even for the $c\bar{s}$ system, $E_{\rm EL}$ is very small. In contrast, our approach, which builds in color separation, yields significant values for $E_{\rm EL}$ for all the mesons in Table II. This, of course, is the origin of the quark mass difference mentioned previously.

TABLE II. Predictions of the present work [$\alpha(1\text{ fm})=1.0$, $\Lambda=0.240$ GeV, $E_0=-1.84/R_0$] for the masses $M_{\rm cal}$ of heavy vector mesons are compared to experimental values $M_{\rm exp}$. The zero-point, volume, and electric contributions to these masses and the expectation values of $\langle p^2/m^2\rangle$ are given. Results of the fixed-bag calculations of Refs. 2 and 5 are also shown. All masses are in GeV.

Approximation	$q\bar{q}$ system	$M_{\rm exp}$	$M_{\rm cal}$	$\langle E_0\rangle$	$\langle E_{\rm VOL}\rangle$	$\langle E_{\rm EL}\rangle$	$\langle p^2/m^2\rangle$
Adiabatic (present work)	$b\bar{b}(m_b=5.26)$	$\Upsilon(9.460)$	9.460	−0.816	0.034	−0.668	0.072
	$c\bar{b}$		6.339	−0.669	0.056	−0.528	
	$b\bar{s}$		5.431	−0.539	0.100	−0.373	
	$c\bar{c}(m_c=1.87)$	$\Psi(3.095)$	3.095	−0.604	0.073	−0.456	0.178
	$c\bar{s}$	$F^*(2.150)$	2.106	−0.519	0.110	−0.343	
	$s\bar{s}(m_s=0.64)$	$\phi(1.020)$	1.020	−0.480	0.137	−0.279	0.563
Fixed bag (Refs. 2, 5)	$c\bar{c}(m_c=1.55)$		3.095	−0.520	0.082	0.0	
	$c\bar{s}$		2.099	−0.446	0.131	0.015	
	$s\bar{s}(m_s=0.28)$		1.068	−0.399	0.183	0.0	

IV. DISCUSSION

From Fig. 9 we see that the wave functions of the various ψ and Υ states are concentrated at quite different values of the q-$\bar{q}$ separation, and consequently are sensitive to appreciably different values of the running coupling constant. Thus, in principle, the spectroscopy and leptonic decay widths of these states provide an ideal test of the variation of the coupling constant with distance.

However, in interpreting experimental data, one must be sure to take into account all the important physics. Of particular relevance to the present bag-model calculations is the increased importance of couplings to decay channels at higher excitation energies. Such couplings, which will both shift the energies of these states and give them widths, have been ignored in our work. If the states in charmonium above 4 GeV are omitted from our calculations, then choosing $\Lambda = 0.375$ GeV in Eq. (2) and fixing γ so that $\alpha(1\text{ fm}) = 2.2$ yields a reasonable fit to the remaining $c\bar{c}$ and $b\bar{b}$ states, provided the c- and b-quark masses are chosen appropriately (see Figs. 7 and 8). In addition, the corresponding ratios of leptonic decay widths $\Gamma(\psi' \to e^+e^-)/\Gamma(\psi \to e^+e^-) = 0.544$ and $\Gamma(\Upsilon' \to e^+e^-)/\Gamma(\Upsilon \to e^+e^-) = 0.489$ are not in serious disagreement with experiment, 0.4 ± 0.1 and 0.3 ± 0.2, respectively.

In view of this we must evaluate our decision to use $\alpha(1\text{ fm}) = 1.0$ rather than the value 2.2 employed in the original fixed-bag fit to the light hadrons.[2] (In that work α is a constant and the characteristic size of bag radii and interquark separations is 1 fm.) Three points should be stressed. First, it is unclear from the work of Ref. 2 how uncertain the value of 2.2 is, or how α is correlated with the other bag parameters. Second, we have found that the choice $\alpha(1\text{ fm}) = 1.0$ not only removes the large discrepancies in the masses of the $3s$, $2d$, and $4s$ states in charmonium, but also improves the agreement with the masses and leptonic decay rates of the lower states. (The masses of the $2s$ and $3s$ states of the b-$\bar{b}$ system are predicted well in both cases.) The final point is an apparent problem with the slope of the Regge trajectories for light hadrons if our asymptotic value for α of 1.1 is taken at face value. For a rotating tube of flux,[23] $\alpha = 1.1$ leads to a Regge slope of 1.2 GeV^{-2}, which is larger than the accepted value. However, it is apparent from Fig. 10 that known $c\bar{c}$ and $b\bar{b}$ states provide little information on the behavior of $\alpha(r)$ above 1.5 fm. Thus we have the freedom to rectify the apparent difficulty with the Regge slope, while changing our present results only slightly, by gradually increasing $\alpha(r)$ in order that a more suitable asymptotic value be reached.

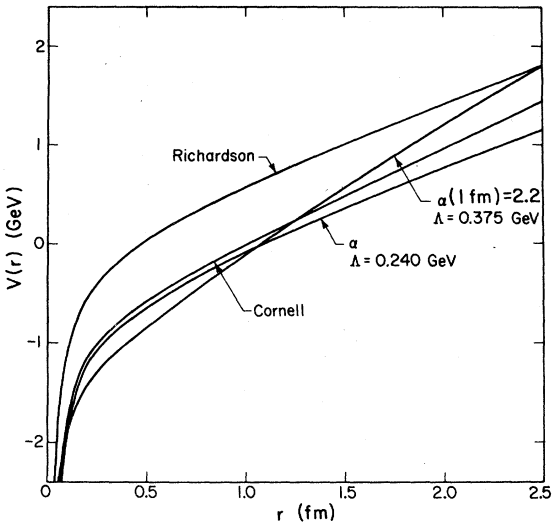

FIG. 11. Potentials derived in the present work for $\alpha(1\text{ fm}) = 1.0$ and $\alpha(1\text{ fm}) = 2.2$ are compared with phenomenological treatments by Richardson (Ref. 18) and by the Cornell group (Ref. 24).

We should also compare phenomenological treatments of the q-$\bar{q}$ potential to our potentials. In Fig. 11 we show $V(r)$ for $\alpha(1\text{ fm}) = 1.0$ and $\alpha(1\text{ fm}) = 2.2$ along with the potential of Richardson,[18] which smoothly interpolates between a linear confining potential at large distances and a form consistent with asymptotic freedom at small distances. (The interpolation was actually performed in momentum space and then Fourier transformed.) Richardson's success in reproducing the $c\bar{c}$ and $b\bar{b}$ spectra and leptonic decay widths is comparable to ours. Indeed, from Fig. 11 we see that beyond q-$\bar{q}$ separations of 0.2 fm, Richardson's potential is remarkably similar to ours with $\alpha(1\text{ fm}) = 1.0$, with the difference approximately a constant 0.68 GeV. This difference is largely absorbed into his quark masses, $m_c = 1.49$ GeV and $m_b = 4.88$ GeV, so that his mass contributions to meson energies are smaller than ours by approximately 0.77 GeV. At small separations our treatment differs from Richardson's due to his scale parameter ($\Lambda = 0.398$ GeV) and to our inclusion of a zero-point energy $-Z_0/R_0(r)$.

There have also been a number of studies of heavy mesons using a very simple phenomenological potential of the form

$$V(r) = -\frac{\kappa}{r} + \frac{r}{a^2} + V_0 , \tag{20}$$

where κ, a, and V_0 are constants. This can be contrasted with Eq. (14). In Fig. 11 one such potential, from the Cornell group,[24] is shown where the constants have the values $\kappa = 0.52$, $a = 2.34$

GeV^{-1}, and $V_0 = -0.84$ GeV. This potential is remarkably similar to one we have derived. This value of V_0 corresponds to the Cornell treatment of charmonium; for the $b\bar{b}$ system the value of V_0 was arbitrarily changed to -0.71 in Ref. 24.

In summary, the quark-antiquark potential which we have determined from an adiabatic approximation to the MIT bag model has proved quite successful in reproducing the masses and leptonic decay widths of heavy vector mesons. This approach nicely complements the earlier fixed-bag approximation which, while quite successful in describing the light hadrons, failed to predict the spectrum of charmonium. We believe that heavy meson spectra can provide a great deal of information on the variation of the running coupling constant with distance. To demonstrate that we have a quantitative understanding of this variation, however, would require a set of parameters in the bag model capable of simultaneously describing heavy-quark systems and light-quark systems. Thus the need for a weaker coupling constant at $r = 1.0$ fm than in the light-hadron calculations and the effects of the opening of decay channels on our analysis remain important questions for further study.

ACKNOWLEDGMENTS

We would like to thank A. T. Aerts, W. Fischler, T. J. Goldman, K. Johnson, J. Kiskis, and A. I. Sanda for helpful conversations. We would also like to thank L. Rosen for permission to use the LAMPF computer facilities. This work was supported by the U. S. Department of Energy.

APPENDIX

In this appendix we present expressions for ϕ and $\vec{\nabla}\phi$, and discuss some numerical difficulties in evaluating these expressions for interior points very near the bag surface.

Completing the azimuthal integral in Eq. (9) we find

$$4\pi\phi(\vec{x}) = \frac{g}{x[(\cos\theta - d/x)^2 + \sin^2\theta]^{1/2}} - \frac{g}{x[(\cos\theta + d/x)^2 + \sin^2\theta]^{1/2}} + 4G\int S(\theta')\sin\theta' R(\theta') d\theta' \frac{1}{(A+B)^{1/2}} \left\{ \frac{C+H}{A-B} E\left[\left(\frac{2B}{A+B}\right)^{1/2}\right] - \frac{2H}{A+B} D\left[\left(\frac{2B}{A+B}\right)^{1/2}\right] \right\}, \tag{A1}$$

where

$$A = x^2 + R(\theta')^2 - 2xR(\theta')\cos\theta\cos\theta', \quad B = 2xR(\theta')\sin\theta\sin\theta',$$

$$C = R(\theta')^2 - xR(\theta')\cos\theta\cos\theta' - x\frac{dR(\theta')}{d\theta'}\cos\theta\sin\theta', \quad H = -xR(\theta')\sin\theta\sin\theta' + x\frac{dR(\theta')}{d\theta'}\sin\theta\cos\theta',$$

$$E(z) = \int_0^{\pi/2} dy (1 - z^2\sin^2 y)^{1/2}, \quad D(z) = \int_0^{\pi/2} dy \frac{\sin^2 y}{(1 - z^2\sin^2 y)^{1/2}}.$$

The q-$\bar{q}$ separation is $2d$ and the radius of the bag is $R(\theta)$.

The corresponding expression for $\vec{\nabla}\phi$ is

$$\begin{aligned} 4\pi\vec{\nabla}\phi(\vec{x}) = {} & \hat{r}_0 \left[\frac{g(x + d\cos\theta)}{[(x\cos\theta + d)^2 + x^2\sin^2\theta]^{3/2}} - \frac{g(x - d\cos\theta)}{[(x\cos\theta - d)^2 + x^2\sin^2\theta]^{3/2}} \right] \\ & - \hat{\theta}_0 gd\sin\theta \left[\frac{1}{[(x\cos\theta - d)^2 + x^2\sin^2\theta]^{3/2}} + \frac{1}{[(x\cos\theta + d)^2 + x^2\sin^2\theta]^{3/2}} \right] \\ & + \hat{r}_0 \frac{2G}{x} \int S(\theta')\sin\theta' R(\theta') \frac{1}{(A+B)^{1/2}} \frac{1}{A-B} \\ & \times \left\{ E\left(\left(\frac{2B}{A+B}\right)^{1/2}\right) \left[\frac{[R(\theta')^2 - x^2][3(AC+BH) + AH + BC]}{A^2 - B^2} - 2R(\theta')^2 - C - H \right] \right. \\ & \left. + \frac{2}{A+B} D\left(\left(\frac{2B}{A+B}\right)^{1/2}\right) \left[H(A-B) - \frac{(AH+BC)[R(\theta')^2 - x^2]}{A+B} \right] \right\} \\ & + \hat{\theta}_0 \frac{2G}{x} \int S(\theta')\sin\theta' R(\theta') \frac{1}{(A+B)^{1/2}} \frac{1}{A-B} \\ & \times \left\{ E\left(\left(\frac{2B}{A+B}\right)^{1/2}\right) \left[-\frac{\partial A}{\partial\theta}\left(\frac{3(AC+HB) + AH + BC}{A^2 - B^2}\right) + 2\frac{\partial C}{\partial\theta} + \frac{\partial B}{\partial\theta}\left(\frac{3(BC+AH) + BH + AC}{A^2 - B^2}\right) \right] \right. \\ & \left. + \frac{2}{(A+B)^2} D\left(\left(\frac{2B}{A+B}\right)^{1/2}\right) \left[(AH+BC)\frac{\partial A}{\partial\theta} - (HB+AC)\frac{\partial B}{\partial\theta} \right] \right\}. \end{aligned} \tag{A2}$$

Some care must be taken in evaluating these expressions for points near the surface since the integrand in Eqs. (A1) and (A2) become very sharply peaked. We have treated this by evaluating analytically the most singular term in Eq. (A1) and the two most singular terms in Eq. (A2). Although the resulting expressions are too complicated to reproduce here, they can be obtained from us on request. The numerical integration scheme employed is an adaptive Newton-Cotes method yielding a maximum relative error of 0.1%.

[1]A. Chodos *et al.*, Phys. Rev. D 9, 3471 (1974).

[2]T. DeGrand *et al.*, Phys. Rev. D 12, 2060 (1975).

[3]P. Hasenfratz, J. Kuti, and A. S. Szalay, *in Charm, Color, and the J/ψ*, proceedings of the X Rencontre de Moriond, Méribel-les-Allues, France, 1975, edited by J. Trân Thanh Vân (CNRS, Paris, 1975); P. Hasenfratz and J. Kuti, Phys. Rep. 40C, 75 (1978).

[4]L. Heller and K. Johnson, Phys. Lett. 84B, 501 (1979).

[5]R. L. Jaffe and J. Kiskis, Phys. Rev. D 13, 1355 (1976).

[6]J. F. Donoghue and K. Johnson [Phys. Rev. D 21, 1975 (1980)] point out that correcting the improper treatment of translational invariance in the original bag-model calculation leads to a term in the energy which is also proportional to $1/R_0$. Note that in the present calculations the potential energy depends only on the separation of the quark and antiquark, and therefore satisfies translational invariance.

[7]K. Johnson [Report No. SLAC-PUB-2436, 1979 (unpublished)] shows that there are contributions to the zero-point energy of the Yang-Mills fields which are proportional to the running coupling canstant, so that Z_0 itself varies with the size of the bag.

[8]A question can be raised as to whether the separation of the quark and antiquark is the correct distance variable to use in the asymptotic freedom formula [Eq. (1)]. If one chose instead some dimension of the bag, this would not simply amount to a different choice of the scale constant Λ because $r\sim$ (radius of bag)^3 for small separations [see Eq. (18)]. Since the Feynman diagram consisting of single gluon exchange between the quark and antiquark has a running coupling constant which presumably is a function of the square of the gluon's momentum, then the potential in momentum space behaves like $[q^2\ln(q^2/\Lambda^2)]^{-1}$ for $q=|\vec{q}|\to\infty$. The Fourier transform of such a potential is *precisely* $[r\ln(1/\Lambda^2r^2)]^{-1}$ in the limit $r\to 0$, with no extra numerical factor. Hence we argue that r is the correct variable. (A specific example of such a potential is given in Ref. 18).

[9]T. Appelquist and J. Carazzone, Phys. Rev. D 11, 2856 (1975).

[10]It can be shown no surface equivalent to S^n, where n is even, has a unit tangent vector field; see D. Husenmoller, *Fibre Bundles* (Springer, New York, 1966), Chap. 11.

[11]R. Giles, Phys. Rev. D 18, 513 (1978).

[12]This error measure is, to an extent, arbitrary. We have not attempted to address the mathematical problem of defining an optimal measure in terms of some convergence criterion. We have, however, found little sensitivity to changes in relative weightings of the two terms in Eq. (10).

[13]We have tried a second form for $\alpha(r)$ which approaches its asymptotic value at a different rate. This form also could not describe the higher states in charmonium when we required $\alpha(1\text{ fm})=2.2$.

[14]A. T. Aerts and L. Heller (unpublished).

[15]K. Johnson, in *Current Trends in the Theory of Fields*, proceedings of the Conference, Tallahassee, 1978, edited by J. E. Lannutti and P. K. Williams (AIP, New York, 1978), p. 112.

[16]Since we have only the central part of the potential, the eigenvalue we determine should lie between the triplet- and singlet-state masses. However, for heavy quarks the splitting of these states is small. For consistency we choose always to compare to the triplet-state masses, which are displaced less than the singlet masses by the noncentral components of the potential.

[17]R. Van Royen and V. Weisskopf, Nuovo Cimento 50, 617 (1967).

[18]J. L. Richardson, Phys. Lett. 82B, 272 (1979).

[19]T. Appelquist, R. M. Barnett, and K. Lane, Annu. Rev. Nucl. Part. Sci. 28, 387 (1978).

[20]G. Flugge, in *Proceedings of the 19th International Conference on High Energy Physics, Tokyo, 1978*, edited by S. Homma, M. Kawaguchi, and H. Miyazawa, (Phys. Soc. of Japan, Tokyo, 1979), p. 793.

[21]If we extend this model still further to the nonstrange quarks, we find $\langle p^2/m^2\rangle = 0.84$.

[22]G. C. Barbarino, in *Gauge Theories and Leptons*, proceedings of the XIII Rencontre de Moriond, Les Arcs, France, 1978, edited by J. Trân Thanh Vân (Editions Frontieres, Gif-Sur-Yvette, 1979), p. 161.

[23]K. Johnson, Acta Phys. Pol. B6, 865 (1975).

[24]E. Eichten *et al.*, Phys. Rev. D 21, 203 (1980).